Supporting Information

Methods

Device fabrication The Si substrate with 300 nm thermal oxide (Nova electronic Materials, Ltd.) was patterned with photolithography to create 100 by100 μm 5/45 nm thick Cr/Au squares as back gate electrodes coated with 10±5 nm Si_3N_4 dielectrics layer by plasma enhanced chemical vapor deposition. The thin Si_3N_4 dielectrics layer was characterized to have only ~ pA leakage current/V and the breakdown voltage >9V at 5 K. Cadmium telluride tetrapod s with ~8 nm wide and ~150 nm long arms capped with octyldecyl phosphonic acid and trioctyl phosphine oxide in toluene were spin-deposited onto the substrate with pre-patterned alignment markers fabricated by e-beam lithography (JEOL 6400 scanning electron microscope (SEM) equipped with Nabity lithography systems) on top of the Au square back gate area. The individual tetrapods were well separated with an area density of ~1-10 /μm^2. The position of tetrapods was located with respect to the alignment markers under SEM. Using the low SEM acceleration voltage (<5 kV) and low beam current is necessary to avoid damaging to the tetrapods. The substrate was then spin-coated (4000 rpm for 60 s) with double layers of electron beam resist: first methyl methacrylate-methacrylic acid copolymer (MMA-MAA) and then 950 KD polymethyl methacrylate (PMMA) from Microchem Inc., followed by 150 °C oven bake for 2 hrs. Electron-beam lithography and electron-beam evaporation was used to define 60 nm thick Pd metal contacts onto the individual tetrapods. The ~30 nm alignment accuracy was routinely achieved to ensure high yield contact to the tetrapods.

Conduction mechanism The energy level spacing for electron and hole is calculated as 45 meV and 5 meV, respectively. The electron energy level spacing already

exceeds the experimental addition energy of 30 meV. This is therefore inconsistent for transport through conduction band, while conforms with transport through the closely spaced valence band levels which are also closely spaced due to band-mixing effects well known for the II-VI semiconductor nanocrystals. The I-V curves of Pd metal contact measured at room temperature is linear. Palladium has a high work function of ~5.2 eV suggesting Fermi level is most likely in the valence band of the tetrapods. For comparison, we also tried Ti as contact metal (~4.4eV work function) and the I-V measurements show >1 eV zero-current voltage gap at room temperature, suggesting the Fermi level is probably in the band-gap. In addition, previous study on CdSe quantum dots covered by similar surfactants and contacted with high work function Au (5.3 eV) electrode also indicate that it is hole transport (Ref. 1). In the future, we will perform study using a powerful gate so that we can move the Fermi level into the bandgap region and determine unambiguously whether it is valence or conduction band.

Charging energy of arm and nanorod The charging energy can be estimated using the gate capacitance value $C=2\pi L\varepsilon\varepsilon_0/\ln(4h/D)$ and the gate coupling efficiency, where L is the effective length of the arm and rod taking into account the metal electrode screening, h is the gate dielectrics thickness ~10 nm, and D is the diameter of the arm and nanorod).

Figure 1. Reproducibility of tetrapod measurements with the third arm floated. Current (I) plotted against bias voltage (V) across two arms of a tetrapod while the third arm was floated. Floating the third arm avoids an additional current pathway. The gate was fixed at 0V and the temperature was 26 K, under which single electron charging can be clearly observed. Green, black and red curves were taken at time 0, 3 hr and 6 hr. The three I-V curves nearly overlap indicating the floated third arm does not induce significant potential drift. The data in Fig. 3 of the main text were taken over 30 min, also indicating the device stability. The data in Fig. 4 of the main text show that a current resonant peak versus V_g with or without the third arm floating is at the same position, suggesting the stability of our devices.

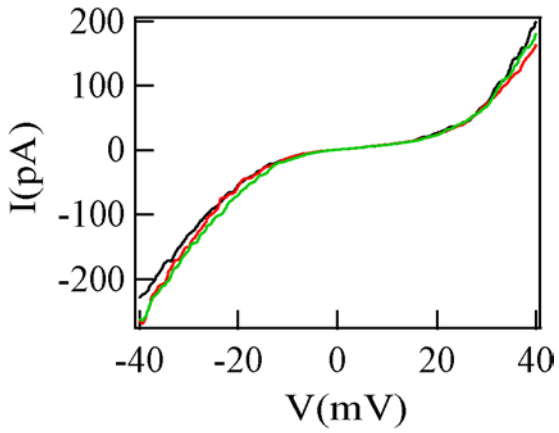

Figure 2. Plot of $\partial I/\partial V$ as function of V and V_g without correcting the sudden charge jumps. The two jumps are indicated by arrows. To produce Fig. 2b of the main text, the right side of the plot to the arrows is shifted left along the V_g axis to preserve the continuity of the line.

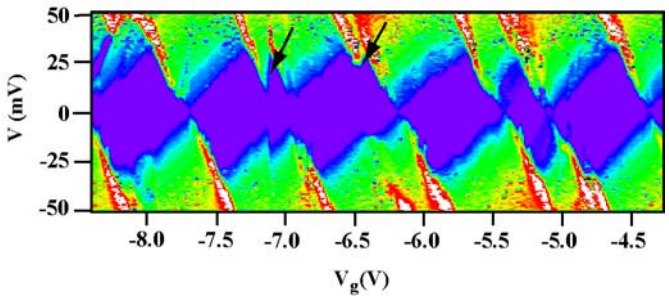

Figure 3. The current (I) as a function of V_g with V= 1 mV is plotted at different temperatures for a tetrapod device exhibiting hopping coupling. The curves are shifted in the vertical axis for clarity. With temperature increased from 4.5 to 28 K, the number of Coulomb oscillation peaks is increased. This can be explained by the three charging energy ladders model of the tetrapods exhibiting weak coupling. It is easier to have three charging levels lining up within a higher temperature window.

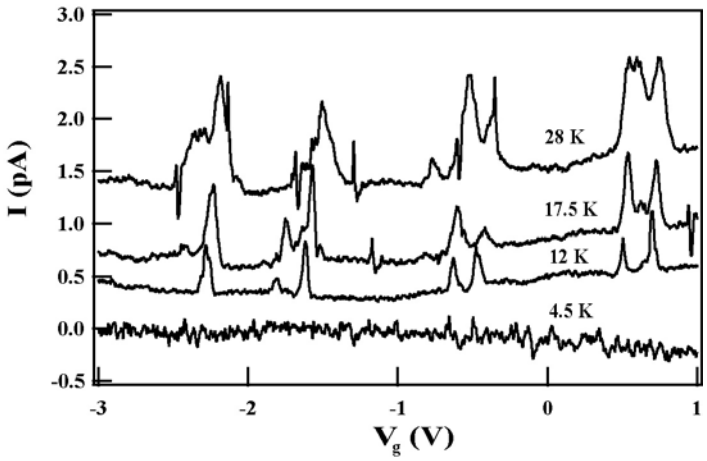

Figure 4. The circuit diagram of a tetrapod. The circuit consists of arm-branch point-arm current pathway and the third floating arm. The capacitances are extracted from the charge stability plot shown in Fig. 2a according to the method in Ref. 22. The arm gate capacitance $C_g=e/V_g$ is estimated to be 2.7aF using the 60 mV V_g separation of the saw-teeth. Similarly, the gate capacitance of the branch point is estimated to be 0.56 aF. The total capacitance of the arm (C_{arm}) or branch point (C_{point}) is calculated from their charging energy e^2/C_{arm}, or e^2/C_{point}, respectively. The other capacitance can be deduced from the slope of the Coulomb diamond boundary. The tunnel resistances are assumed to be the same as 50 MOhm across the metal-arm and arm-core interfaces, which will give the total resistance of 200 MOhm consistent with the resistance out of the Coulomb blockade region in Fig. 2a.

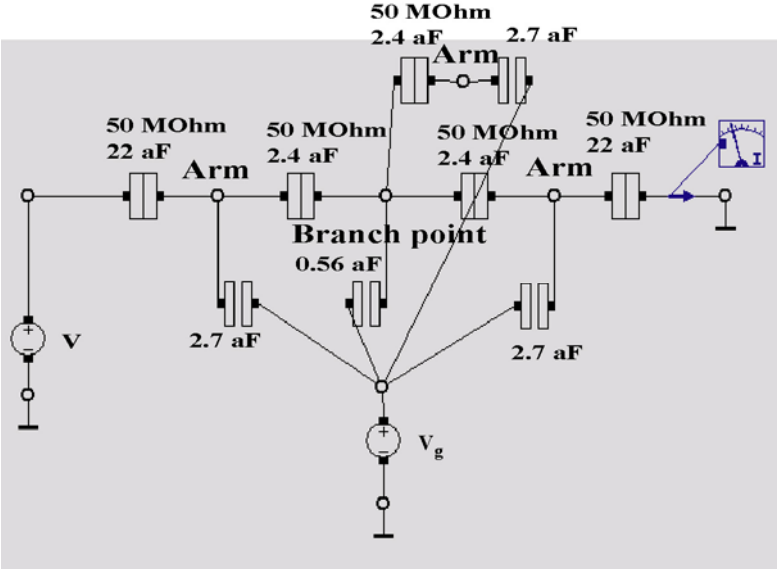

Figure 5. Plot of current (I) as function of the third arm gate corresponding to I versus time plot in Fig. 4b. Label 1 to 3 have the same meaning as in Fig. 4 of the main text (1, 2, 3 correspond to the different V_g values: 1, current blockade; 2, current at the half maximum of the Coulomb oscillation peak; 3, current at the top of the peak.).

.